Supplemental Information for:

Multifunctional photoresponsive organic molecule for electric field sensing and modulation

Yingmu Zhang[a], Jinghan He[b], Patrick J.G. Saris[a], Hyun Uk Chae[c], Subrata Das[c], Rehan Kapadia[c], Andrea M. Armani [a b c] *

Table of Contents

1 Synthesis of NAI-TPE-PyS

Materials

All commercially available chemical reagents and solvents including 1,8-naphthalic anhydride, ammonia, 1,10-dibromodecane 4-bromoiodobenzene, 4-Formylphenylboronic acid, bis(pinacolato)diboron, tetrakis(triphenylphosphine)palladium ($Pd(PPh_3)_4$), [1,1′-Bis(diphenylphosphino)ferrocene]dichloropalladium(II) ($Pd(dppf)Cl_2$), 4-Picoline, 1,3-propanesulton, piperidine, potassium carbonate (K_2CO_3), potassium acetate (KOAc), anhydrous sodium sulfate (Na_2SO_4), *N*,*N*-Dimethylformamide (DMF), dimethyl sulfoxide (DMSO), dichloromethane (DCM), chloroform, Tetrahydrofuran (THF), methanol (MeOH), ethanol (EtOH), ethyl acetate, hexane were either purchased from VWR or Sigma Aldrich. Unless otherwise noted, they were used without further purification. 1H-benz[de]isoquinoline-1,3(2H)-dione (1) and 4,4′-(2-(4-Bromophenyl)-2-phenylethene-1,1-diyl)- diphenol (5) were synthesized based on previously published procedures with modifications, as indicated.

^{1}H and ^{13}C NMR spectra were recorded on a Varian Mercury 400 MHz spectrometer with 96-spinner sampler changer using either deuterated chloroform or DMSO as solvent, as indicated.

Synthesis overview

Scheme S1 shows the overview of the entire synthesis process for the NAI-TPE-PyS molecule. Compound 2, Compound 6, and Compound 8 are combined to form the desired product.

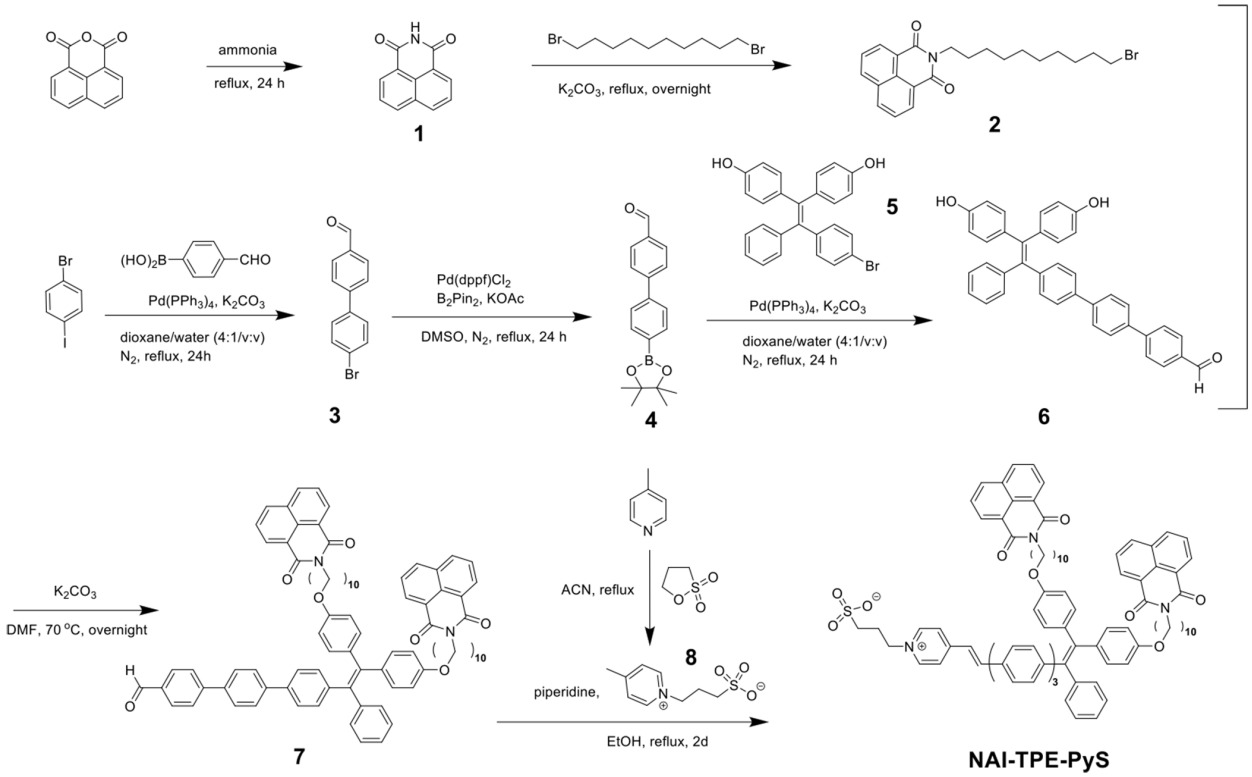

Scheme S1. Synthetic scheme of NAI-TPE-PyS.

Synthesis of 2-(10-Bromodecyl)-1H-benz[de]isoquinoline-1,3(2H)-dione (Compound 2)

Compound **1** was synthesized according to the previously published procedure.[1]

Into a 250 mL double-neck round-bottom flask was added **1** (2.0 g, 10.1 mmol) and dry *N*,*N*-Dimethylformamide (DMF, 80 mL). The mixture was stirred at 60°C for 12h to make **1** fully dissolved. Then, K_2CO_3 (2.79 g, 20.2 mmol) and 1,10-Dibromodecane (15.15 g, 50.5 mmol) were added, and the system was allowed to react at 60°C for another 24 h. After finishing, K_2CO_3 was removed by filtration, and the solvent was removed under vacuum. The crude product was further purified by silica column chromatography with ethyl acetate : hexane (1:9/v:v) as eluent to yield a white solid.

^{1}H NMR (400 Hz, Chloroform-*d*): δ 8.61 (d, J = 7.2 Hz, 2H), 8.21 (d, J = 8.1 Hz, 2H), 7.76 (t, 2H), 4.18 (t, 2H), 3.40 (t, J = 7.0 Hz, 2H), 1.84 (p, J=7.0 Hz, 2H), 1.74 (p, J=7.5 Hz, 3H), 1.47 = 1.24 (m, 12H). ^{13}C-NMR (101MHz, Chloroform-d): *δ*: 164.20, 133.83, 131.58, 131.16, 128.16, 126.91, 122.77, 40.47, 34.04, 32.83, 29.38, 29.34, 29.27, 28.71, 28.15, 28.09, 27.09.

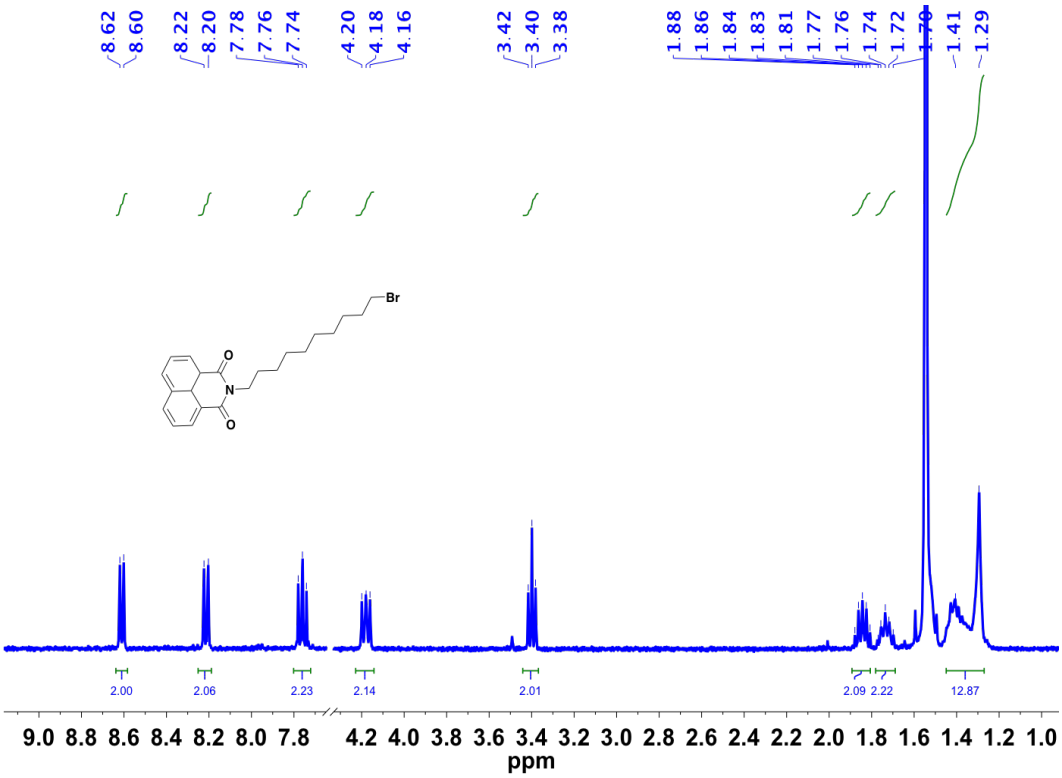

Fig. S1. [1]H NMR of 2-(10-Bromodecyl)-1H-benz[de]isoquinoline-1,3(2H)-dione.

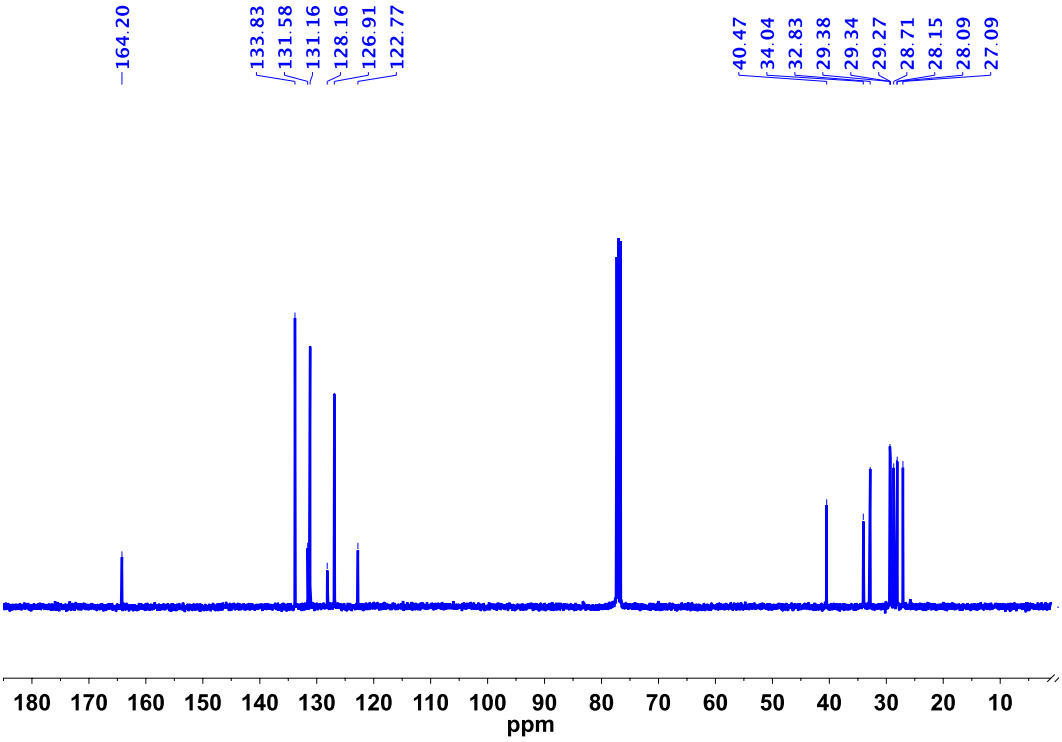

Fig. S2. [13]C NMR of 2-(10-Bromodecyl)-1H-benz[de]isoquinoline-1,3(2H)-dione.

Synthesis of 1-(4-Bromophenyl)-2,2-bis(4-hydroxyphenyl)-1-phenylethene (Compound 3)

Into a 250 mL round-bottom flask were added 4-Bromoiodobenzene (20 mmol, 5.66 g), 4-Formylphenylboronic acid (20 mmol, 3.0 g), $Pd(PPh_3)_4$ (0.52 mmol, 600 mg) and K_2CO_3 (7.0g, 50 mmol). The flask was fitted on the Schlenk line, vacuum evacuated, and refilled with nitrogen alternately three times. A mixing solvent (dioxane/water: 80 mL/20 mL) was bubbled with nitrogen for 30 min and then transferred to the flask through a canula. The mixture was then allowed to react for 12 hours at 80 °C. After cooling to the room temperature, the mixture was poured into water and extracted with DCM three times. The combined organic part was dried with sodium sulfate, and the solvent was removed by vacuum. The obtained solid was then purified by column chromatography with eluent ethyl acetate : hexane (1: 10/v:v) to give a white powder.

^{1}H NMR (400 MHz, Chloroform-*d*) δ 10.07 (s, 1H), 7.95 (s, 2H), 7.71 (s, 2H), 7.62 (d, *J* = 8.6 Hz, 2H), 7.51 (d, *J* = 8.6 Hz, 2H). ^{13}C-NMR (101MHz, Chloroform-d): δ 191.76, 145.88, 138.61, 135.45, 132.18, 130.35, 128.90, 127.49, 122.95.

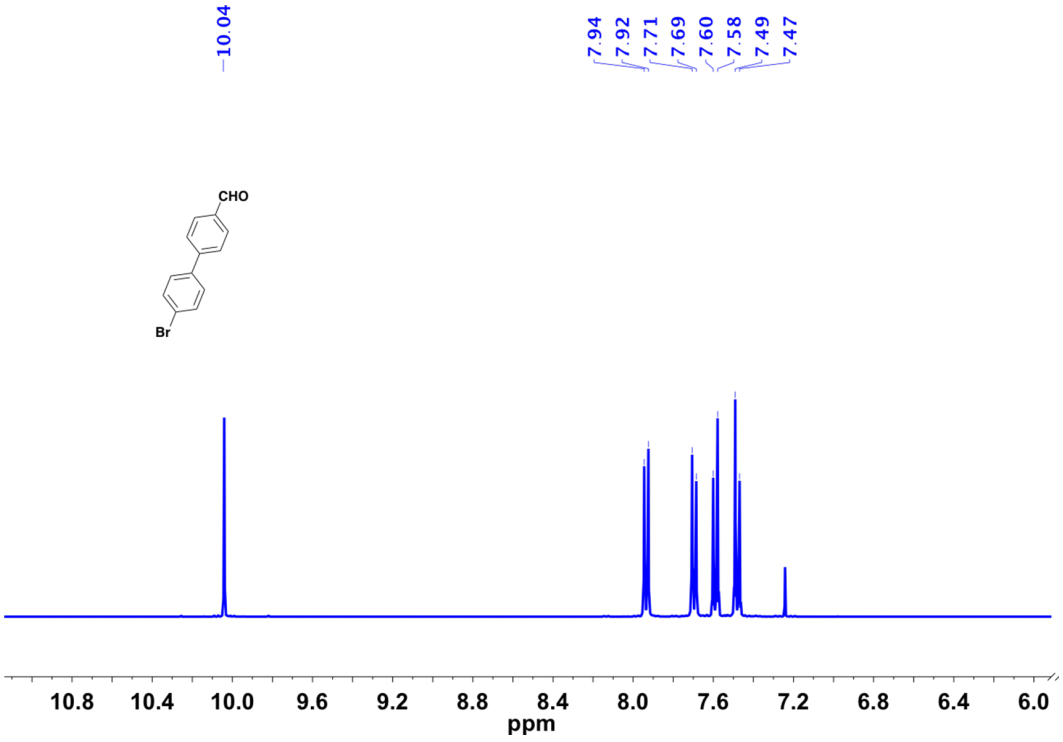

Fig. S3. ^{1}H NMR of 1-(4-Bromophenyl)-2,2-bis(4-hydroxyphenyl)-1-phenylethene.

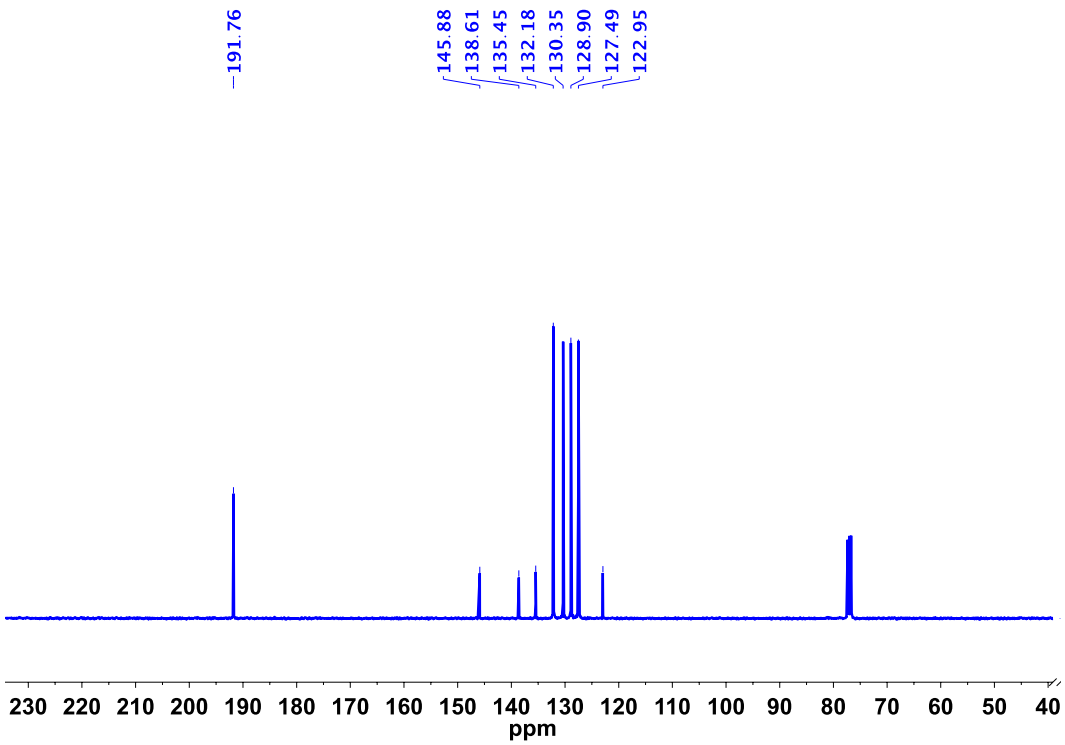

Fig. S4. ^{13}C NMR of 1-(4-Bromophenyl)-2,2-bis(4-hydroxyphenyl)-1-phenylethene.

Synthesis of 4'-(4,4,5,5-tetramethyl-1,3,2-dioxaborolan-2-yl)-[1,1'-biphenyl]-4-carbaldehyde (Compound 4)

Compound **3** (1.0 g, 3.8 mmol), bis(pinacolato)diboron (1.5 g, 5.7 mmol), KOAc (1.2 g, 11.4 mmo) and Pd(dppf)Cl_2 (150 mg, 0.2 mmol) were added to a 250 mL Schleck flask with a stir bar. The flask was pumped under vacuum and refilled with N_2 three times before 50 mL degased DMSO was transferred to the system. The solution mixture was then heated at 100 ^{0}C overnight under N_2. After cooling to room temperature, the mixture was poured into 200 mL of DI water, extracted with DCM twice and then washed with water three times. The combined organic layer was dried by anhydrous Na_2SO_4 and the organic solvent was pumped out. The crude product was then purified by column chromatography on silica gel with ethyl acetate/DCM (1 : 9/v:v) to give compound 4.

^{1}H NMR (400 MHz, Chloroform-*d*) δ 10.07 (s, 1H), 7.95 (s, 2H), 7.71 (s, 2H), 7.62 (d, *J* = 8.6 Hz, 2H), 7.51 (d, *J* = 8.6 Hz, 2H), 1.35 (s, 12 H). ^{13}C-NMR (101MHz, Chloroform-d): δ 191.88, 146.97, 142.24, 135.42, 130.23, 127.79, 126.62, 83.97, 83.48, 25.01, 24.87.

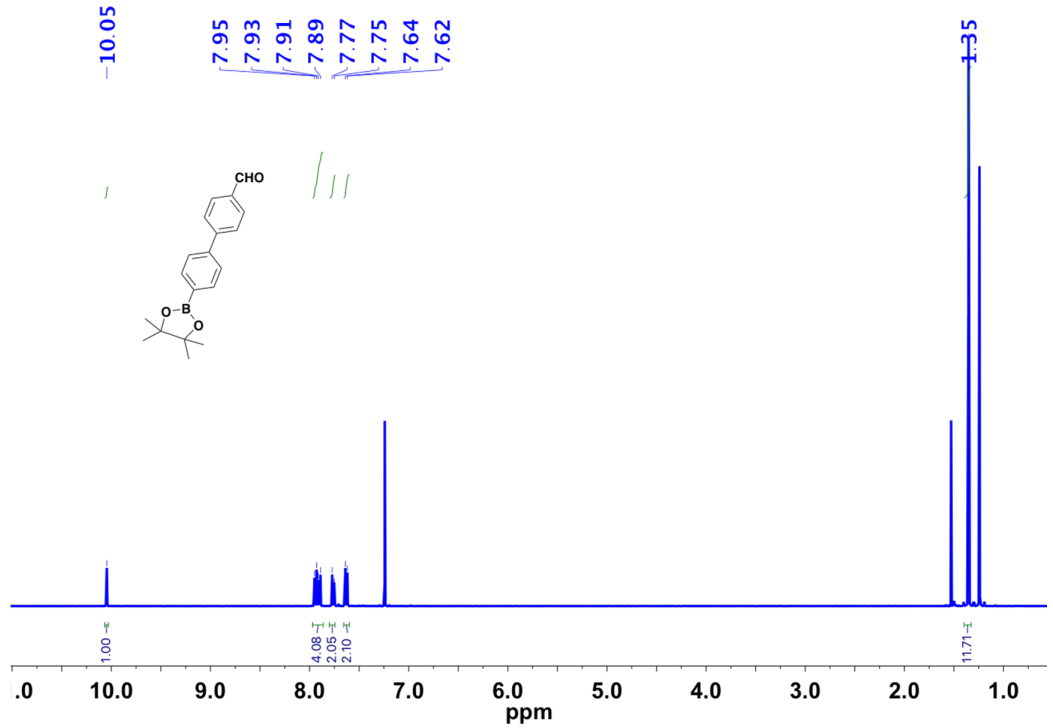

Fig. S5. ^{1}H NMR of 4'-(4,4,5,5-tetramethyl-1,3,2-dioxaborolan-2-yl)-[1,1'-biphenyl]-4-carbaldehyde.

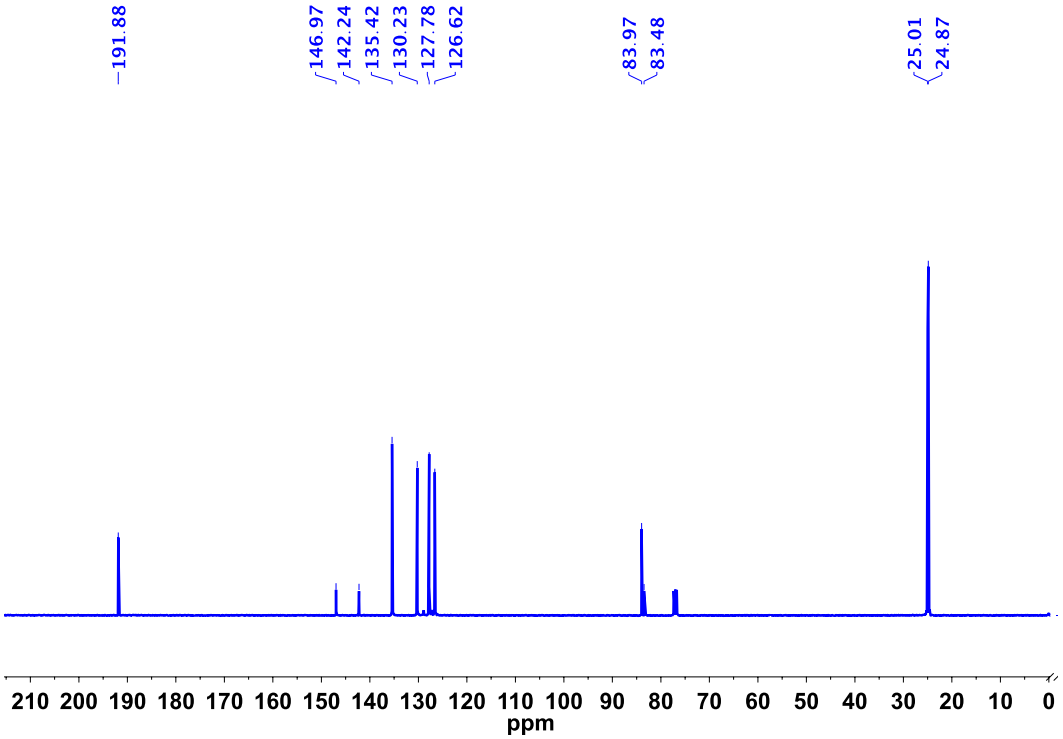

Fig. S6. ^{13}C NMR of 4'-(4,4,5,5-tetramethyl-1,3,2-dioxaborolan-2-yl)-[1,1'-biphenyl]-4-carbaldehyde.

Synthesis of 4''-(2,2-bis(4-hydroxyphenyl)-1-phenylvinyl)-[1,1':4',1''-terphenyl]-4-carbaldehyde (Compound 6)

Compound **5** was synthesized according to previously reported literature.[2] Then, **4** (2.3 mmol, 0.7 g), **5** (1.9 mmol, 0.84 g), $Pd(PPh_3)_4$ (0.19 mmol, 200 mg) and K_2CO_3 (7.6 mmol, 1.05 g) were added into a 100 mL round-bottom flask. The flask was fitted on the Schlenk line, vacuumed and refilled with nitrogen alternately three times. A mixing solvent (dioxane/water: 40 mL/10 mL) was bubbled with nitrogen for 30 min and then transferred to the flask through a canula. The mixture was then allowed to react for 24 hours at 100 °C. After cooling to room temperature, the mixture was poured into DI water and the pH was adjusted to about 5. Then, the system was extracted with DCM and washed with water three times. The organic solvent was then removed and the crude solid was recrystallized by hexane/ DCM to give the pure product.

^{1}H NMR (400 MHz, Chloroform-*d*) δ 10.06 (s, 1H), 7.96 (d, *J* = 8.1 Hz, 2H), 7.79 (d, *J* = 8.4 Hz, 2H), 7.68 (s, 4H), 7.41 (d, *J* = 8.2 Hz, 3H), 7.12 (d, *J* = 2.2 Hz, 4H), 7.06 (s, 2H), 6.93 (dd, *J* = 16.6, 8.5 Hz, 4H), 6.59 (t, *J* = 9.0 Hz, 4H). ^{13}C-NMR (101MHz, Chloroform-d): 191.91, 154.22, 154.14, 146.48, 144.10, 143.74, 140.85, 140.34, 138.79, 137.56, 136.40, 135.16, 132.78, 131.90, 131.42, 130.32, 127.75, 127.64, 127.46, 127.37, 126.22, 126.13, 114.68, 114.56.

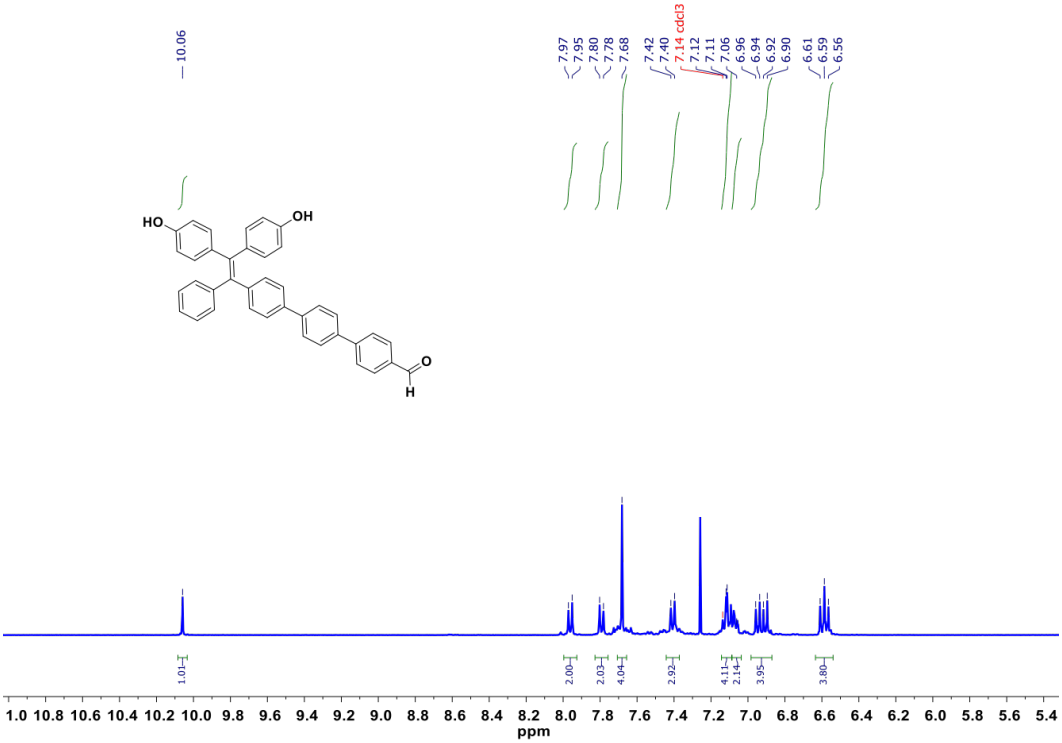

Fig. S7. ^{1}H NMR of (Z)-4''-(1,2-bis(4-hydroxyphenyl)-2-phenylvinyl)-[1,1':4',1''-terphenyl]-4-carbaldehyde.

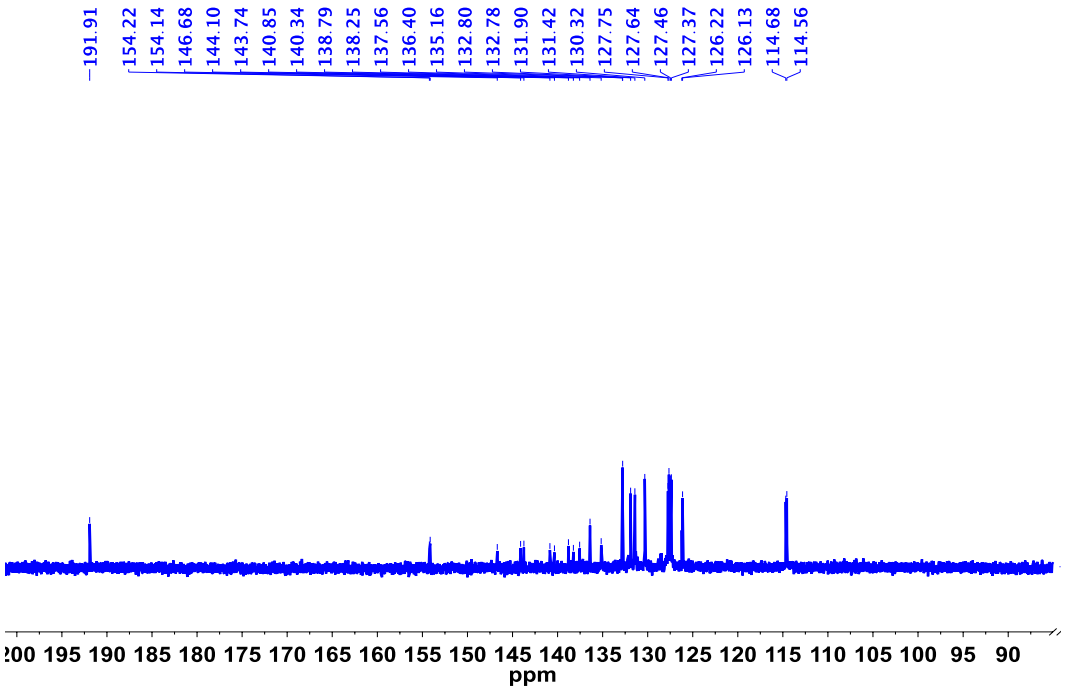

Fig. S8. ^{13}C NMR of (Z)-4''-(1,2-bis(4-hydroxyphenyl)-2-phenylvinyl)-[1,1':4',1''-terphenyl]-4-carbaldehyde.

Synthesis of 4''-(2,2-bis(4-((10-(1,3-dioxo-1H-benzo[de]isoquinolin-2(3H)-yl)decyl)oxy)phenyl)-1-phenylvinyl)-[1,1':4',1''-terphenyl]-4-carbaldehyde (NAI-TPE-CHO, Compound 7)

Into a 250 mL two-necked round-bottom flask was added K_2CO_3 (248.8 mg, 1.8 mmol), **2** (500 mg, 1.2 mmol) and **6** (163 mg, 0.3 mmol). The flask was vacuumed and purged with dry N_2 three times. Then DMF (15 mL) was added and the reaction was stirred overnight at 70 °C. After cooling to room temperature, the mixture was poured into water, extracted with dichloromethane (DCM), washed with distilled water several times and dried with anhydrous magnesium sulfate. The crude product was purified by silica column chromatography with hexane and ethyl acetate (gradient to 1:1/v:v) as eluent to give **7** as a yellow viscous oil (200 mg, 56 %).

^{1}H NMR (400 MHz, Chloroform-d) δ 9.97 (s, 1H), 8.54 – 8.48 (m, 4H), 8.16 – 8.11 (m, 4H), 7.87 (d, J = 8.4 Hz, 2H), 7.74 – 7.63 (m, 7H), 7.60 (s, 4H), 7.32 (d, J = 8.4 Hz, 2H), 7.07 – 6.97 (m, 6H), 6.87 (dd, J = 17.3, 8.8 Hz, 4H), 6.60 – 6.51 (m, 4H), 4.12 – 4.07 (m, 4H), 3.79 (t, J = 6.5 Hz, 4H), 1.71 – 1.59 (m, 8H), 1.28 (d, J = 42.0 Hz, 24H). ^{13}C-NMR (101MHz, Chloroform-d): 191.52, 164.19, 133.83, 132.61, 132.21, 131.56, 131.16, 130.30, 128.13, 127.79, 127.60,

127.42, 127.34, 126.09, 122.73, 113.90, 68.23, 40.48, 32.75, 32.64, 29.38, 29.32, 29.29, 29.28, 28.08, 28.04, 27.09, 26.02, 25.95, 25.78, 25.64.

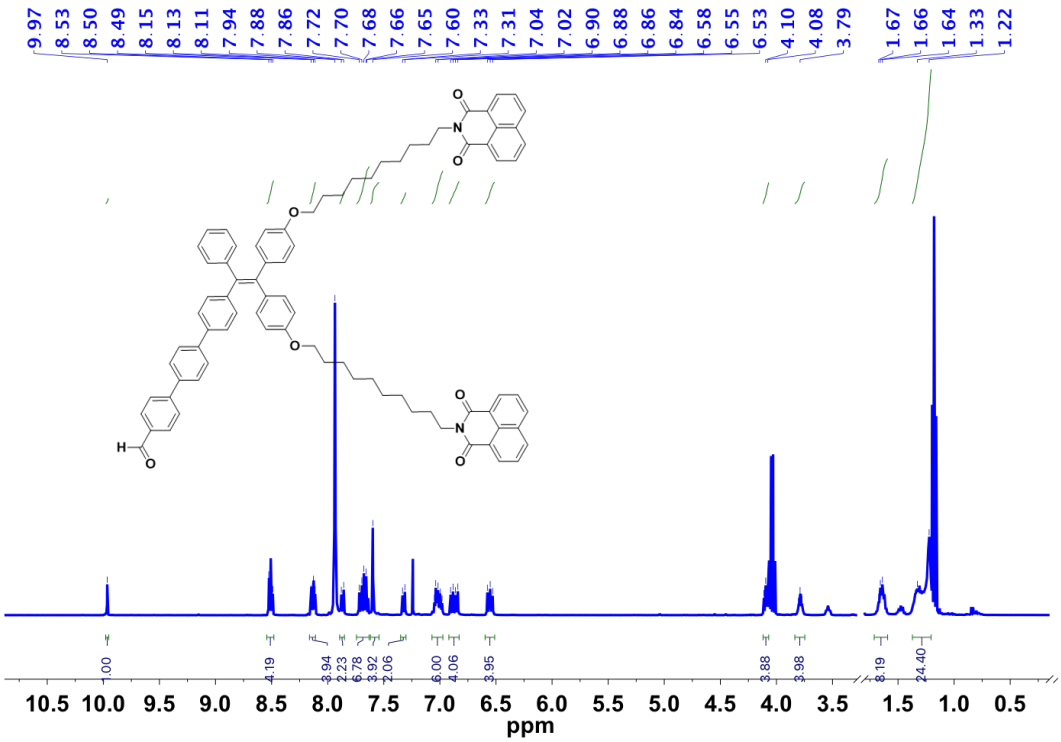

Fig. S9. ^{1}H NMR of NAI-TPE-CHO.

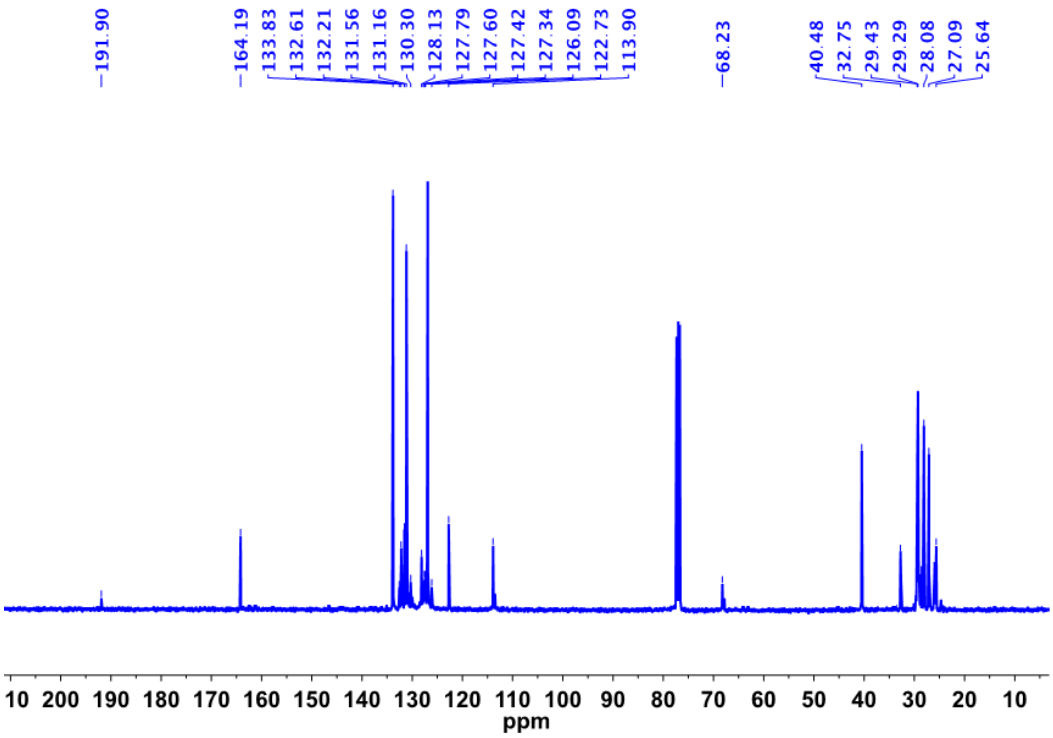

Fig. S10. ^{13}C NMR of NAI-TPE-CHO.

Synthesis of 3-(4-methylpyridin-1-ium-1-yl)propane-1-sulfonate (Compound 8)

4-Picoline (1.8 g, 20 mmol) was dissolved in 15 ml MeCN. 1,3-propanesultone (3.7 g, 30 mmol) was added and the reaction mixture was heated to 80 ºC for 4 hours. After completion, the crude product was precipitated. The solid was filtered and washed with ethyl ether to give compound **8** (86%) as a white solid.

^{1}H NMR (400 MHz, DMSO-d6) δ 8.88 (d, J = 6.8 Hz, 2H), 7.94 (d, J = 6.3 Hz, 2H), 4.63 (t, J = 6.9 Hz, 2H), 2.56 (s, 3H), 2.36 (t, J = 7.2 Hz, 2H), 2.17 (q, J = 6.9 Hz, 2H). ^{13}C NMR (101 MHz, DMSO-d_6) δ 159.21, 144.37, 128.78, 59.22, 47.38, 27.69, 21.82.

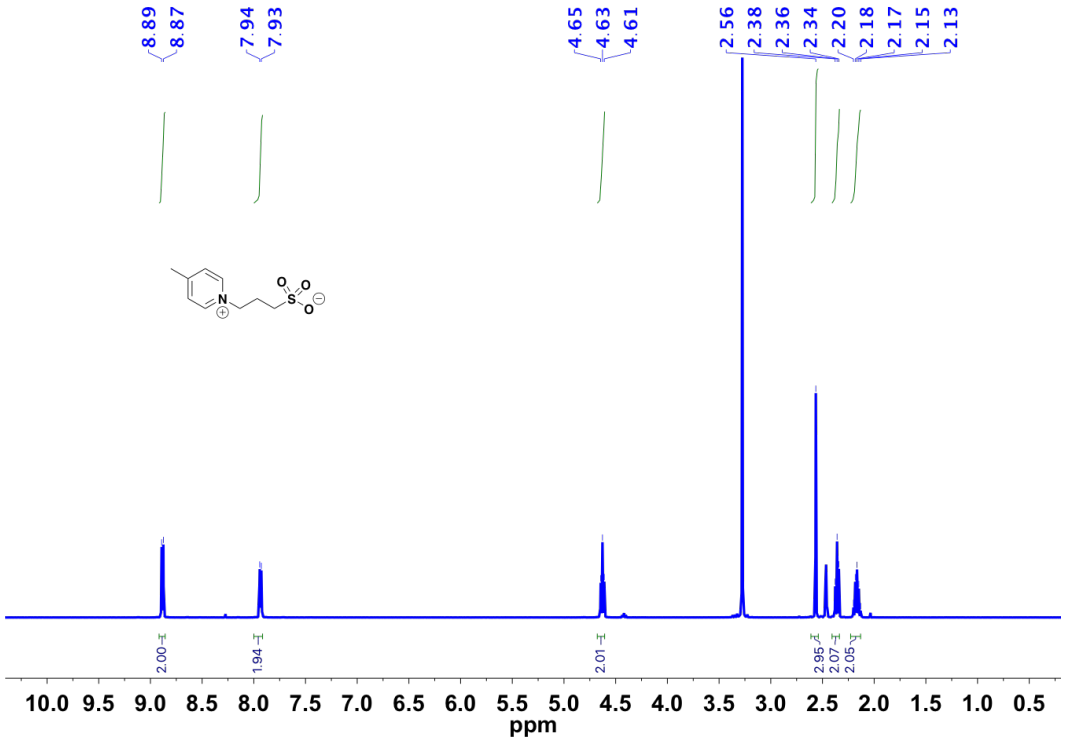

Fig. S11. ^{1}H NMR of 3-(4-methylpyridin-1-ium-1-yl)propane-1-sulfonate.

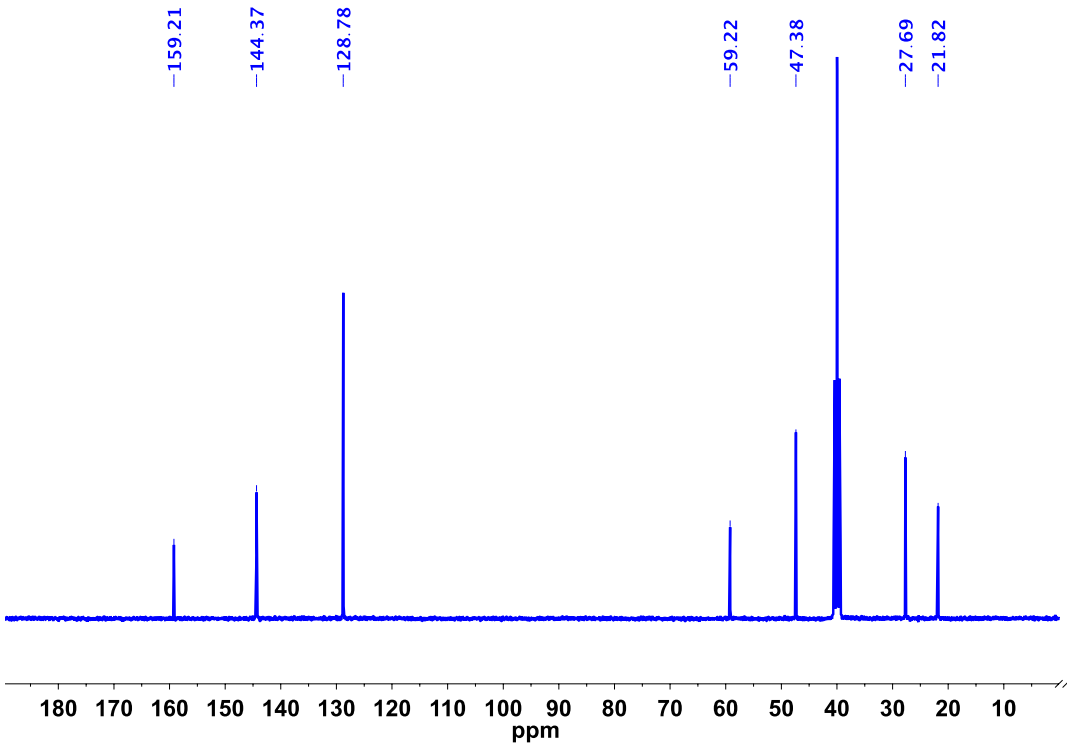

Fig. S12. ^{13}C NMR of 3-(4-methylpyridin-1-ium-1-yl)propane-1-sulfonate.

Synthesis of (E)-3-(4-(2-(4''-(2,2-bis(4-((10-(1,3-dioxo-1H-benzo[de]isoquinolin-2(3H)-yl)decyl)oxy)phenyl)-1-phenylvinyl)-[1,1':4',1''-terphenyl]-4-yl)vinyl)pyridin-1-ium-1-yl)propane-1-sulfonate (NAI-TPE-PyS)

A mixture solution of **7** (300 mg, 0.25 mmol), **8** (53 mg, 0.25mol), and piperidine catalyst (0.2 mL) was refluxed in 10 mL dry EtOH under N_2 for 48 hrs. The solution turned deep red. After cooling to room temperature, the solvent was removed and the crude solid was purified by column with eluent of DCM: MeOH (10:1/v:v) to give a red solid (83 %).

^{1}H NMR (400 MHz, dmso) δ 9.21 (d, *J* = 6.9 Hz, 1H), 8.94 (d, *J* = 7.2 Hz, 1H), 8.47-8.41 (m, 10H), 8.29 (s, 2H), 8.20 (d, *J* = 7.0 Hz, 2H), 7.86-7.66 (m, 8H), 7.64 (d, *J* = 8.8 Hz, 1H), 7.51 (d, *J* = 8.5 Hz, 1H), 7.10 (dd, *J* = 14.4, 7.3 Hz, 4H), 7.03 – 6.95 (m, 6H), 6.84 (dd, *J* = 22.2, 10.3 Hz, 4H), 6.69 – 6.61 (m, 4H), 4.80 (t, *J* = 6.9 Hz, 2H), 4.20 (t, *J* = 7.0 Hz, 4H), 3.81 (t, *J* = 6.8 Hz, 4H), 2.45-2.41 (m, 2H), 2.22 (t, *J* = 6.9 Hz, 2H), 1.59-1.52 (m, 10H), 1.26-1.19 (m, 22H). ^{13}C NMR (101 MHz, cdcl$_3$) δ 164.12, 163.99, 133.75, 132.84, 131,10, 131.10, 127.57, 127.09, 126.87, 122,68, 56.55, 40.44, 29.68, 29.43, 29.30, 28.07, 27.09, 26.41, 22.66

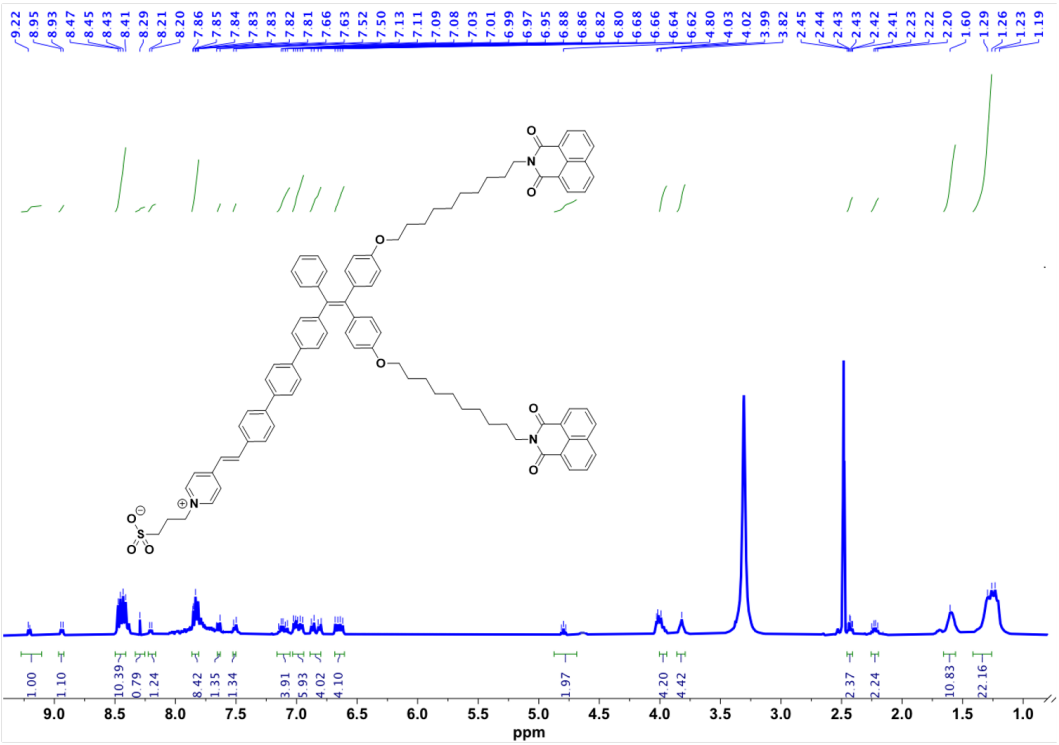

Fig. S13. ^{1}H NMR of NAI-TPE-PyS.

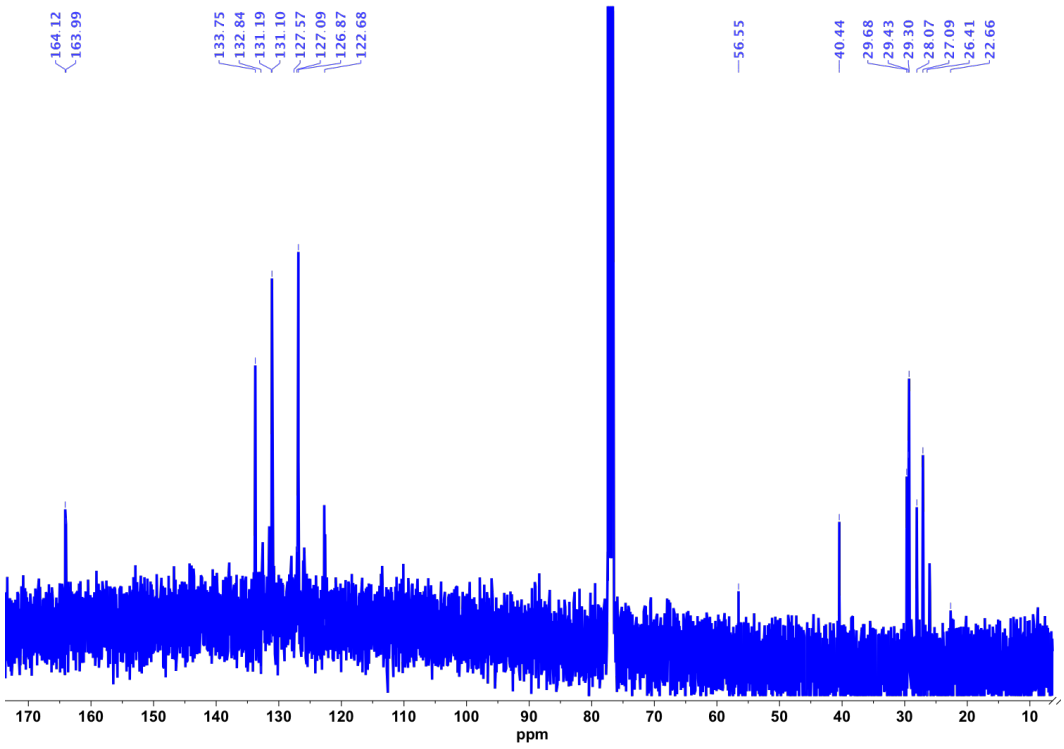

Fig. S14. ^{13}C NMR of NAI-TPE-PyS.

2 Optical Behavior and Photophysical Properties

Dulbecco's phosphate-buffered saline (DPBS, 1X) was purchased from Thermo Fisher Scientific. Selective solvents *N*,*N*-Dimethylformamide (DMF), dimethyl sulfoxide (DMSO), dichloromethane (DCM), chloroform, Tetrahydrofuran (THF), methanol (MeOH), ethanol (EtOH) were either purchased from VWR or Sigma Aldrich.

All UV-Vis absorption spectra were measured on Beckman Coulter Life Science UV/Vis spectrophotometer, DU 730 with wavelength resolution of 2 nm. Steady-state fluorescence spectra were recorded on Horiba Scientific Fluoromax-4 spectrofluorometer with excitation slit width of 5 nm and emission slit width of 5 nm. Quantum yield was determined by a Quanta-φ integrating sphere. Powder sample and aqueous solution of the sample (10 μM, containing 1% DMSO) were prepared for the measurements.

The optical absorption, steady-state emission, and quantum yield were measured under several different conditions to understand the role of pH, solvent polarity, and fluorophore concentration on emission intensity and emission wavelength. Measurements were performed on both solution and thin film samples. Solution samples in selective solvents were prepared by serial dilution to give the desired concentrations, and thin film samples were prepared by dropping DCM solution of NAI-TPE-PyS on Swiss glass slide (size: 25 mm x 75 mm, thick: 1.0 mm) followed by air-dry evaporation.

Fig. S15 shows the UV-Vis absorption measurements of several synthetic precursors, the final product both in DCM and in PBS, and the final product deposited as a thin film on quartz substrate.

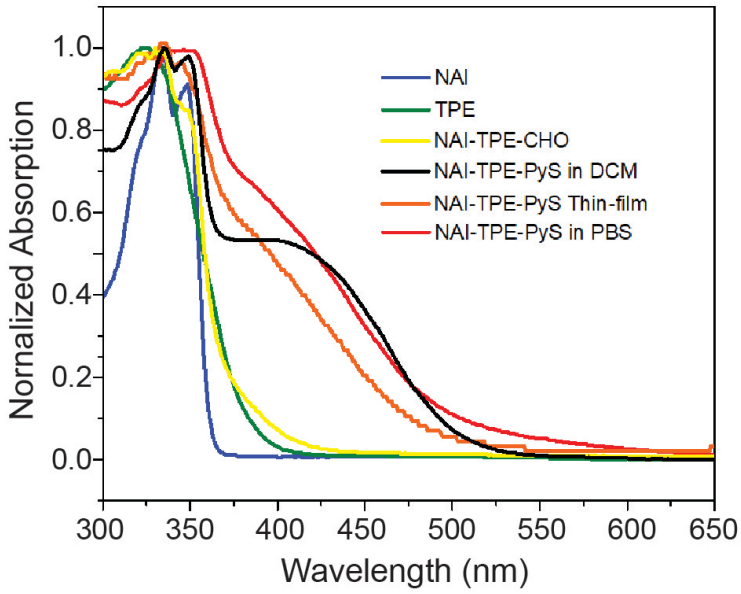

Fig. S15. Absorption Comparison among NAI-TPE-PyS and synthetic precursors in solvents and solid state.

Fig. S16 and Fig. S17 shows the results from a study of the UV-Vis absorption behavior and of the fluorescence behavior of the final product in a range of solvents. The maximum absorption and emission wavelengths for each solvent is summarized in Table S1. Optical images of each solution are shown in Fig. S18.

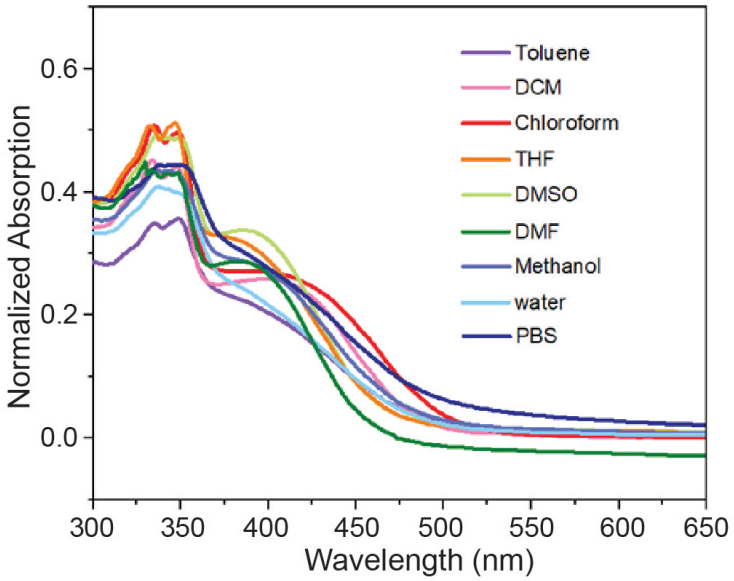

Fig. S16. Absorption spectra of NAI-TPE-PyS in different solvents. Concentration: 10 μM.

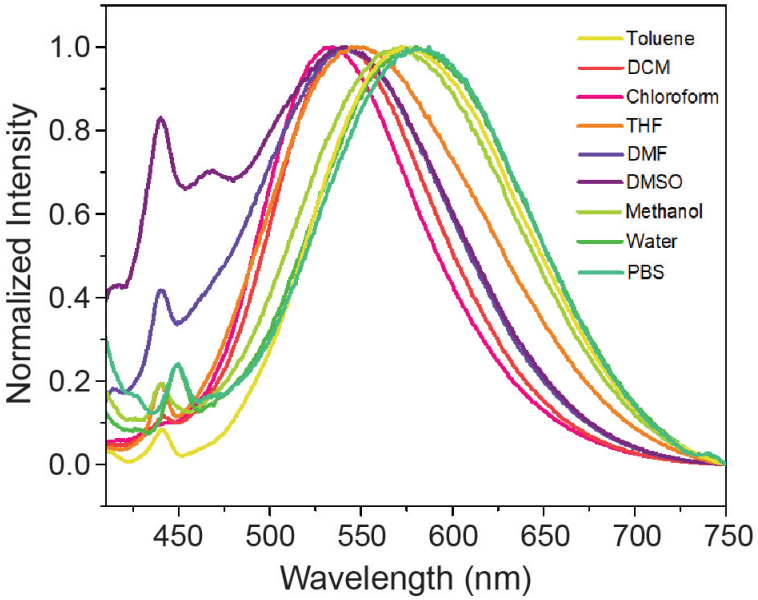

Fig. S17. Emission spectra of NAI-TPE-PyS in different solvents. Concentration: 10 μM, λ_{ex}= 390 nm.

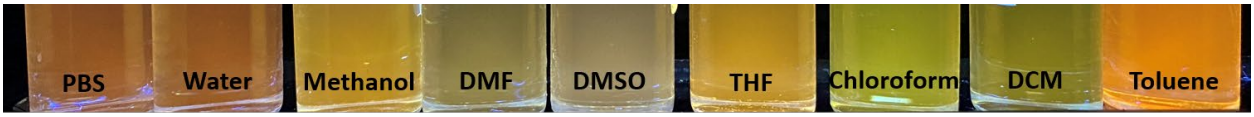

Fig. S18. Photographic images of NAI-TPE-PyS emission in different solvents at λ_{ex}= 365 nm.

Table S1 summarizes the detailed photophysical data of NAI-TPE-PyS in different solvents including orientation polarizability of selective solvents (Δf), λ_{abs} and λ_{em} derived from the UV and FL peaks and calculated ν_{abs}, ν_{em} and Stoke shift ($\nu_{abs}-\nu_{em}$). Figure 19 depicts the Lippert-Mataga relation by plotting Stoke shifts against solvent orientation polarity, showing a positive solvotochromic effect.

The relationship between the Stoke shift ($\nu_{abs}-\nu_{em}$) of the fluorophore and orientation polarizability $f(\varepsilon, n)$ can be described by the Lippert-Mataga equation:

$$hc(\nu_{abs}-\nu_{em}) = hc(\nu^0_{abs}-\nu^0_{em}) + \frac{2(\mu_e-\mu_g)^2}{a^3} f(\varepsilon, n)$$

where h is Plank's constant, c is the velocity of light, f is the orientational polarizability of the solvent, $\nu^0_{abs}-\nu^0_{em}$ corresponds to the Stokes shifts when f is zero, μ_e is the excited-state dipole moment, μ_g is the ground-state dipole moment, a is the solvent Onsager cavity radius derived from Avogadro number (N), molecular weight (M) and density (d =1.0 g/cm^3), and ε and n are the solvent dielectric and the solvent refractive index, respectively.

μ_e can be calculated according to the equation:

$$\mu_e = \mu_g + \left\{\frac{hca^3}{2} * \left[\frac{d(\nu_{abs}-\nu_{em})}{df(\varepsilon, n)}\right]\right\}^{\frac{1}{2}}$$

where μ_g was estimated around 29.3 D from DFT in the gas phase at the B3LYP/6-31g* level of theory 31G(d) level, and μ_e was calculated to be 59.1 D.

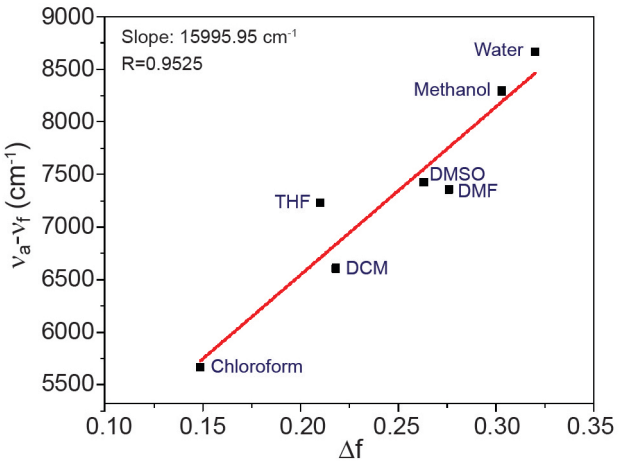

Figure S19. Lippert-Mataga plot for NAI-TPE-PyS in different solvents as a function of solvent polarity. (Δf : orientation polarizability; $\nu_{abs}-\nu_{em}$: Stoke shifts).

Table S1. Detailed photophysical data of NAI-TPE-PyS in selective solvents.

Solvent	Δf	λ_{abs} (nm)	λ_{em} (nm)	ν_{abs} (cm^{-1})	ν_{em} (cm^{-1})	$\nu_{abs}-\nu_{em}$ (cm^{-1})
DCM	0.218	398	540	25125.63	18518.52	6607.11
chloroform	0.149	410	534	24390.24	18726.59	5663.652
THF	0.210	391	545	25575.45	18348.62	7226.824
DMSO	0.263	386	541	25906.74	18484.29	7422.447
DMF	0.276	387	541	25839.79	18484.29	7355.505
Methanol	0.309	388	541	25773.2	17482.52	8290.678
water	0.32	386	580	25906.74	17241.38	8665.356
PBS	_	398	582	25125.63	17182.13	6607.11

3 Aggregation Behaviors

The AIE feature of the compound was studied by adding anti-solvent THF into the DMSO solution of NAI-TPE-PyS (20 μM) gradually with volume fraction ranging from 0% to 99 %. The measurement of AIE property requires an environment where the compound form aggregates or micelles. As NAI-TPE-PyS is well dispersed in DMSO and shows low solubility in

THF, the mixture DMSO/THF are chosen to provide an environment for NAI-TPE-PyS to form aggregates.

The emission intensity of the mixtures was then measured at λex= 390 nm. Figure S20 (a) shows the PL spectra of NAI-TPE-PyS in DMSO/THF mixtures with different THF fractions (f_{THF}), and Fig. S20(b) indicates the corresponding relative PL intensity.

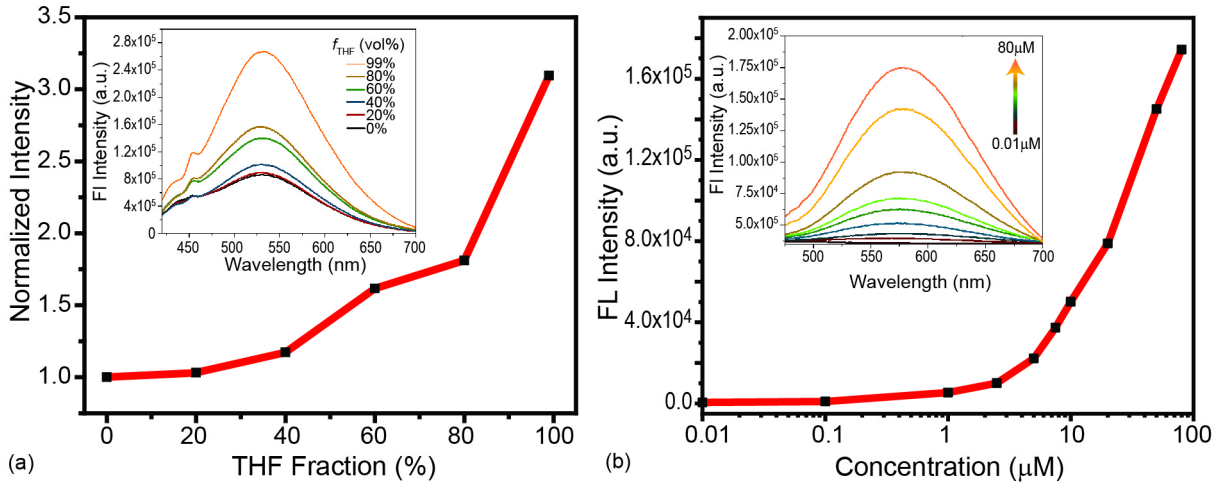

Fig. S20. AIE behavior of NAI-TPE-PyS. (a) Plot of relative PL intensity versus THF fraction. Inset: PL spectra of NAI-TPE-PyS in DMSO/THF mixtures with different THF fractions (f_{THF}). Concentration of NAI-TPE-PyS is 20 μM; λ_{ex}= 390 nm. (b) Plot of PL intensity versus NAI-TPE-PyS concentration in water. Inset: PL spectra of aqueous solutions of NAI-TPE-PyS at concentrations ranging from 0.01μM to 80μM (λ_{ex}= 390 nm).

DLS is used to prove the formation of NAI-TPE-PyS aggregates in aqueous media. DMSO solution of NAI-TPE-PyS (8 mM) was diluted with DI water to give 50 μM sample solution in DMSO/water mixture with water fraction of 99 % (v%). The measurements were conducted on cuvette-based DLS instrument DynaPro®NanoStar®, WYATT Technology. The obtained particle size distribution was plotted in Fig. S21 and particles with effective diameter of 500 nm were given by DYNAMICS® software.

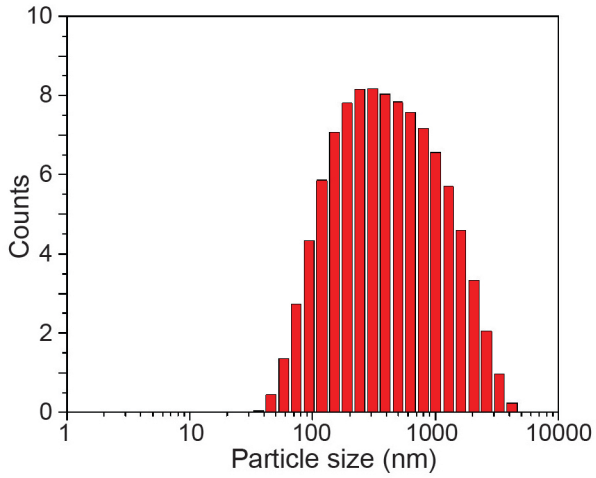

Figure S21. Particle size distribution of NAI-TPE-PyS aggregates in DMSO/THF mixture with a 99% THF fraction. Concentration: 50 μM.

4 Two-photon excitation

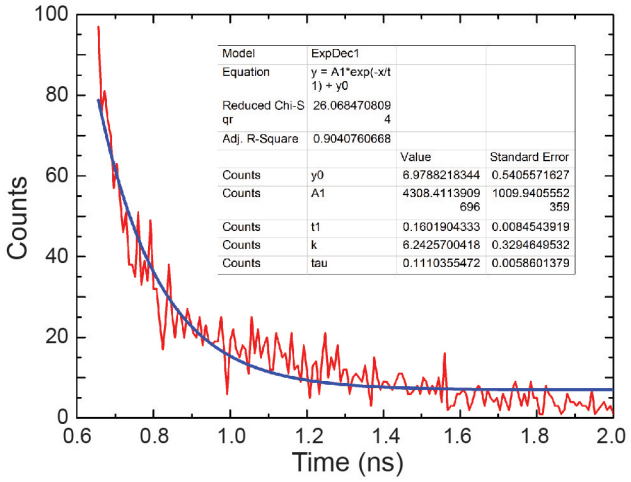

Fig. S22. TCSPC histogram of NAI-TPE-PyS under 750 nm excitation. Red: transient decay trace; Blue: exponential fit line; Inset: exponential fit parameters.

Time-resolved photoluminescence (TRPL) measurements were performed at room temperature using a standard confocal microscope-based Time-Correlated Single Photon

Counting (TCSPC) setup. For this measurement, the sample was dropped cast on a glass slide and a 750 nm pulsed laser (Spectra-Physics, Mai Tai, Mode-Locked Ti:Sapphire Laser) with a pulse width of less than 200 fs and repetition rate of 80 MHz was focused on the sample with a microscope objective. The PL signal from the sample was then passed through two short pass filters with a cut-off wavelength of 550 nm in order to reject the laser light from the laser radiation. Finally, the PL photons were detected with a Si Avalanche Photo Diode (Si-APD) and the PL transient was measured as a function of time. The results are shown in Fig. S22.

5 Photoconductivity

SiO_2/Si (2 μm thermal SiO_2) substrate was cleaned with acetone, IPA and D.I. water. A combination of photolithography, metal deposition, and lift-off were performed to pattern the electrical pad. Photoresist (AZ 5214) was spuncoat for 60 seconds at 3000 rpm, and a standard template mask with channel dimensions of 200 μm (length) x 5000 μm (width) was used as the electrode pattern. 5 nm Ti and 100nm Au was deposited using e-beam evaporation (Temescal, SL1800), and the residual photoresist was lifted-off, completing the electrode fabrication. A thin film of NAI-TPE-PyS was spun-coat on the device from a 6 wt% chloroform solution for 30 s with 500 rpm. Dark and light current measurements were performed by measuring by the voltage across the electrical contact pad. Photoconductivity of the device and I−t measurements were characterized by a Semiconductor Parameter Analyzer (Keysight B1500a). UV light source was provided by DYMAX LED DX-100 with λ_{ex}=350 nm.

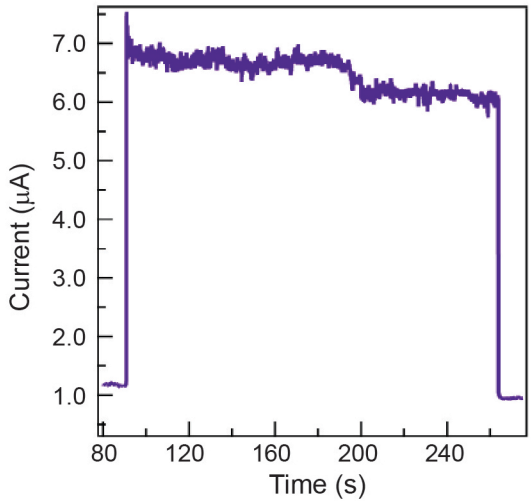

Figure S23. I-t curve of the device at fixed voltage of 10 V upon light illumination with 19 mW optical power.

Table S2. The responsivity studies of our molecules.

Wavelength (nm)	Incident Optical Power (mW)	Responsivity (μA/W)
dark	N/A	0.07
350	8	0.16
350	12.5	0.22
350	16	0.30
350	19	0.41

6 References

1. Streciwilk W*, et al.* Synthesis and Biological Evaluation of Organometallic Complexes Bearing Bis-1, 8-naphthalimide Ligands. *European Journal of Inorganic Chemistry* **2018**, 3104-3112 (2018).

2. Zhao E*, et al.* Light-enhanced bacterial killing and wash-free imaging based on AIE fluorogen. *ACS Appl Mater Interfaces* **7**, 7180-7188 (2015).